INSTITUTE OF PHYSICS PUBLISHING JOURNAL OF PHYSICS B: ATOMIC, MOLECULAR AND OPTICAL PHYSICS

J. Phys. B: At. Mol. Opt. Phys. **39** (2006) 1485–1497 doi:10.1088/0953-4075/39/6/017

R-matrix calculation of the potential energy curves for Rydberg states of carbon monoxide

K Chakrabarti[1] **and Jonathan Tennyson**[2]

[1] Department of Mathematics, Scottish Church College, 1 & 3 Urquhart Sq, Kolkata 700 006, India
[2] Department of Physics and Astronomy, University College London, Gower St, London WC1E 6BT, UK

Received 18 October 2005, in final form 10 February 2006
Published 6 March 2006
Online at stacks.iop.org/JPhysB/39/1485

Abstract

An electron collision formalism is used to consider Rydberg states of the CO molecule as a function of internuclear separation. Up to 14 target states of CO^+ are used in close-coupled expansion and bound states are characterized by searching for negative energy solutions of the scattering calculations. These calculations give potential energy curves for excited states of CO as well as quantum defects as a function of internuclear separation, R. The quantum defects are found to depend only weakly on R except in the region of perturbations caused by intruder states.

(Some figures in this article are in colour only in the electronic version)

1. Introduction

Carbon monoxide is the second most abundant molecule in the universe after molecular hydrogen, due, at least in part, to its large binding energy. Its spectrum is one of the most studied astrophysically, but its large binding energy means that many electronically excited states possess discrete line spectra. Electronic spectra of CO have been extensively studied (Masaki *et al* 1995, Eidelsberg and Rostas 1990, 2003, Ebata *et al* 1992, Drabbels *et al* 1993, Eikema *et al* 1994, Baker *et al* 1995, Komatsu *et al* 1995, Ebata *et al* 1995, Mellinger and Vidal 1995, Mellinger *et al* 1996, 2001, Okazaki *et al* 2001). The astrophysical significance of these spectra has been discussed by Eidelsberg and Rostas (1990, 2003).

Electronically excited states of CO have also been the subject of many theoretical studies using standard *ab initio* procedures, see Kucharskii *et al* (2001) and references therein. However, such methods are not well suited to the study of higher lying electronically excited states which become increasingly diffuse in character. A number of alternative computational procedures have been proposed to study such Rydberg states. These include the polarization propagation method of Nielsen *et al* (1980), a perturbation theory model for molecular Rydberg states developed by Singleton *et al* (1995) and methods based on the direct determination of

Table 1. Excitation energies, T_e in eV, from the X $^2\Sigma^+$ ground state of the CO^+ molecule. For this work these excitations are relative to an absolute energy of $-112.444\,976\ E_h$ at $R_e = 2.132a_0$. $N(\Gamma)$ denotes the number of configurations given by the CAS target model for each target symmetry Γ.

Excited state	Experiment[a]	CCSDT[b]	This work
N $^2\Sigma^+$	320		
X $^2\Sigma^+$	0	0	0
B $^2\Sigma^+$	5.69	5.70	6.56
G $^2\Sigma^+$	–	–	10.30
E $^2\Sigma^+$	–	–	12.47
$N(^2\Sigma^-)$			264
$^2\Sigma^-$	–	–	8.43
$N(^2\Pi)$			486
A $^2\Pi$	2.57	2.55	3.27
D $^2\Pi$	8.40	8.50	8.97
$^2\Pi$	–	–	10.22
$^2\Pi$	–	–	10.88
$^2\Pi$	–	–	11.88
$N(^2\Delta)$			276
C $^2\Delta$	7.81	7.84	8.48
$^2\Delta$	–	–	9.85
$^2\Delta$	–	–	12.70
$N(^4\Sigma^+)$			164
a $^4\Sigma^+$	–	5.68	5.83
$N(^4\Sigma^-)$			196
1 $^4\Sigma^-$	–	7.28	7.76
$N(^4\Pi)$			292
b $^4\Pi$	–	6.98	7.85
$N(^4\Delta)$			152
1 $^4\Delta$	–	6.70	7.16

[a] Huber and Herzberg (1979).
[b] Coupled clusters calculation of Okada and Iwata (2000).

quantum defects (Leyh and Raseev 1986, 1988, Hiyama and Nakamura 1996, Hiyama *et al* 1997). One of us (Tennyson 1996b) used the Rydberg states of CO as a benchmark for testing a new algorithm (Tennyson 1996a) for performing R-matrix calculations. This study was restricted to a single internuclear separation ($R = 2.132a_0$) and was thus of limited use for spectroscopic analysis.

In this work we present calculations on the electronically excited states of CO, particularly the Rydberg states, performed as a function of internuclear separation. These calculations allow us to map out curves for many low-lying Rydberg states of CO. Furthermore, by obtaining values for bondlength-dependent quantum defects, estimates can be made for the potential energy curves of higher Rydberg states.

2. Calculations

2.1. Method

The R-matrix method divides configuration space into two regions (Burke and Berrington 1993). The inner region is defined by a sphere centred at the molecular centre of mass. This sphere encloses the entire N-electron target wavefunction, where for present purposes the

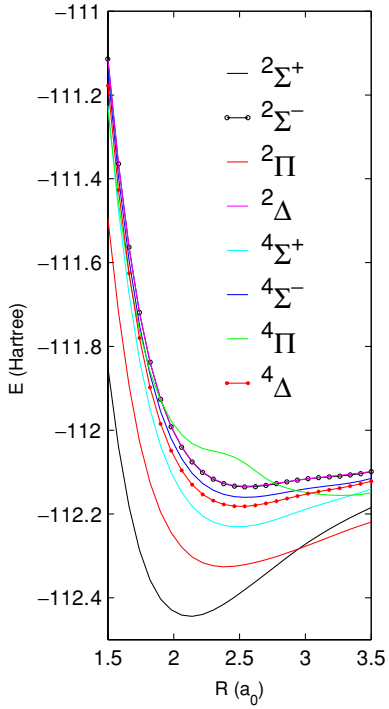

Figure 1. Potential energy curves for the eight lowest states of CO^+ molecule.

Table 2. Number and symmetry of target states used in close-coupling expansion, equation (1), as a function of total symmetry. The lowest energy target state of each symmetry was used in each case.

Symmetry	Number	Target states used
$^1\Sigma^+$	8	Three $^2\Sigma^+$ and $^2\Pi$ states + two $^2\Delta$ states
$^1\Pi$	8	As above
$^1\Sigma^-$	6	$^2\Sigma^-$ state, three $^2\Pi$ and two $^2\Delta$ states.
$^1\Delta$	13	Three $^2\Sigma^+$, $^2\Sigma^-$ and $^2\Pi$ states + four $^2\Delta$ states.
$^3\Sigma^+$	11	Eight states as $^1\Sigma^+$ + one $^4\Sigma^+$, $^4\Pi$ and $^4\Delta$ states
$^3\Pi$	13	11 states as above + one $^2\Sigma^-$ and $^4\Sigma^-$ states
$^3\Sigma^-$	13	Three $^4\Sigma^-$, $^2\Pi$ and $^2\Delta$ states + two $^4\Pi$ and $^4\Delta$ states.
$^3\Delta$	14	Three $^2\Sigma^+$, $^2\Sigma^-$, $^2\Pi$, $^2\Delta$ states + one $^4\Sigma^+$ and $^4\Delta$ state.

'target' means CO^+. In this inner region, the wavefunction of the $(N + 1)$-electron system, CO, is given by

$$\Psi_k = \mathcal{A} \sum_{i,j} a_{i,j,k} \Phi_i(1, \ldots, N) F_{i,j}(N + 1) + \sum_i b_{i,k} \chi_i(1, \ldots, N + 1), \qquad (1)$$

where $\mathcal{A}$ is the antisymetrization operator, $F_{i,j}$ are continuum orbitals and χ_i are two-centre L^2 functions constructed from N-electron 'target' orbitals.

In (1), Φ_i is the wavefunction of the ith target state. Electron-correlation effects are included in these target wavefunctions via configuration interaction (CI) expansions. As discussed extensively in Tennyson (1996b), the choice of this CI expansion largely determines which L^2 functions are included in the wavefunction.

Table 3. Vertical excitation energies, in eV, from the X $^1\Sigma^+$ ground state of the CO molecule at $R_e = 2.132a_0$.

Excited state	This work	Experiment[a]	Theory			
			CCSDT[b]	RPA[c]	SPP (1)[c]	SPP (2)[c]
I $^1\Sigma^-$	11.32	9.88	10.05	9.35	10.34	9.74
B $^1\Sigma^+$	10.57	10.78	10.98	12.00	11.06	10.96
C $^1\Sigma^+$	11.13	11.40	–	12.68	11.61	11.54
F $^1\Sigma^+$	12.06	12.4	–	14.19	13.02	12.82
Y $^1\Sigma^+$	12.24	>12.4	–	14.87	13.77	13.52
e $^3\Sigma^-$	10.70	9.88	–	9.35	10.25	9.64
a' $^3\Sigma^+$	9.32	8.51	–	6.33	8.79	8.02
b $^3\Sigma^+$	10.20	10.4	–	11.18	10.70	10.58
j $^3\Sigma^+$	11.04	11.3	–	12.42	11.53	11.43
g $^3\Sigma^+$	12.00	>12.2	–	14.22	13.25	13.13
h $^3\Sigma^+$	12.17	>12.5	–	14.66	13.99	13.87
A $^1\Pi$	9.26	8.51	8.54	8.89	8.96	8.53
E $^1\Pi$	11.23	11.53	–	12.71	11.54	11.65
V $^1\Pi$	12.17	>12.30	–	13.91	13.03	13.18
G $^1\Pi$	12.45	>12.50	–	14.80	13.50	13.47
G' $^1\Pi$	12.76	>12.5	–	15.17	13.75	13.68
a $^3\Pi$	6.55	6.32	–	5.35	6.54	6.02
c $^3\Pi$	11.13	11.55	–	12.51	11.64	11.55
3 $^3\Pi$	12.16	–	–	13.22	11.80	11.82
4 $^3\Pi$	12.41	–	–	13.74	13.20	13.07
5 $^3\Pi$	12.76	–	–	14.89	13.75	13.64
D $^1\Delta$	10.87	10.23	10.18	9.93	10.46	9.95
d $^3\Delta$	10.31	9.36	–	7.90	9.69	8.96

[a] Huber and Herzberg (1979).
[b] Kucharskii *et al* (2001).
[c] Nielsen *et al* (1980).

2.2. CO^+ target

Calculations on both CO^+ and CO were performed for ten internuclear distances in the range 1.5–3.5a_0. The CO Slater-type orbitals of Kirby-Docken and Liu (1977) were used to build a CO^+ molecular basis of 46 molecular orbitals (24σ, 14π, 6δ, 2ϕ). An initial set of molecular orbitals was obtained by performing self-consistent field (SCF) calculations on the two lowest states of CO^+, X $^2\Sigma^+$ and A $^2\Pi$. These SCF molecular orbitals were then used in a configuration interaction (CI) calculation. In all calculations the 1σ, 2σ molecular orbitals were frozen and the CI calculation used the following configurations:

$$(3\sigma,4\sigma, 5\sigma, 1\pi)^9,$$
$$(3\sigma,4\sigma, 5\sigma, 1\pi)^8\ (6\sigma - 24\sigma, 2\pi - 14\pi, 1\delta - 6\delta)^1,$$
$$(3\sigma,4\sigma, 5\sigma, 1\pi)^7, (6\sigma - 24\sigma, 2\pi - 14\pi, 1\delta - 6\delta)^2.$$

These correspond, respectively, to a complete active space (CAS) spanning valence orbitals, single excitations from this CAS and double excitations. Two sets of pseudo-natural orbitals (NOs) were obtained from CI calculation on the lowest CO^+ states with $^2\Sigma^+$ and $^2\Pi$ symmetry described above. Following Tennyson (1996b), all σ and the 1π orbitals in the target state wavefunction were represented by $^2\Sigma^+$ NOs, and the remaining π and all δ orbitals were represented by the $^2\Pi$ NOs

Table 4. Comparison of quantum defects for the low-lying singlet Rydberg states of the CO molecule. Theory results are for $R_e = 2.132a_0$.

	Experiment				Theory		
State	a	b	c	d	e	f	g
$3s\sigma$ B $^1\Sigma^+$	0.95	–	0.950	–	1.084	0.92	0.853
$4s\sigma$ J $^1\Sigma^+$	0.92	0.921	0.921	0.920	1.054	0.87	0.845
$5s\sigma$ I′ $^1\Sigma^+$	–	–	0.943	0.934	1.043	0.86	0.842
$6s\sigma$ $^1\Sigma^+$	–	–	0.913	0.908	1.035	0.85	0.840
$3p\sigma$ C $^1\Sigma^+$	0.72	0.720	0.720	–	0.684	0.65	0.625
$4p\sigma$ K $^1\Sigma^+$	0.67	0.683	0.683	–	0.666	0.62	0.615
$5p\sigma$ $^1\Sigma^+$	–	0.675	0.671	0.669	0.657	0.61	0.610
$6p\sigma$ $^1\Sigma^+$	–	0.658	0.666	0.666	0.653	0.61	0.607
$3d\sigma$ F $^1\Sigma^+$	0.13	0.127	0.126	–	0.014	0.01	0.043
$4d\sigma$ $^1\Sigma^+$	0.14	–	0.137	–	0.013	0.01	0.046
$5d\sigma$ $^1\Sigma^+$	0.15	–	0.146	–	0.030	0.01	0.047
$4f\sigma$ $^1\Sigma^+$	–	–	–	0.017	–	–	0.007
$5f\sigma$ $^1\Sigma^+$	–	–	–	0.020	–	–	
$6f\sigma$ $^1\Sigma^+$	–	–	–	0.020	–	–	0.008
$3p\pi$ E $^1\Pi$	0.66	0.663	0.664	–	0.656	0.52	0.582
$4p\pi$ L $^1\Pi$	0.67	0.647	0.646	–	0.623	0.53	0.582
$5p\pi$ $^1\Pi$	–	0.656	0.595	0.582	0.610	0.53	0.582
$6p\pi$ $^1\Pi$	–	0.644	0.645	0.638	0.604	0.54	0.581
$7p\pi$ $^1\Pi$	–	0.622	–	0.595	0.598	–	0.581
$3d\pi$ G $^1\Pi$	−0.03	−0.024	−0.024	–	−0.019	−0.09	−0.069

[a] Hammond *et al* (1985).
[b] Ogawa and Ogawa (1972), Ogawa and Ogawa (1974).
[c] Eidelsberg and Rostas (1990).
[d] Komatsu *et al* (1995).
[e] Singleton *et al* (1995).
[f] Hiyama and Nakamura (1996), Hiyama *et al* (1997).
[g] This work.

Table 5. Comparison of quantum defects for the low-lying triplet Rydberg states of the CO molecule. Theory results are for $R_e = 2.132a_0$.

	Experiment			
State	a	b	c	This work
$3s\sigma$ b $^3\Sigma^+$	1.06	–	–	0.931
$4s\sigma$ h $^3\Sigma^+$	1.05	1.053	–	0.918
$3p\sigma$ j $^3\Sigma^+$	0.77	–	0.776	0.668
$4p\sigma$ $^3\Sigma^+$	–	–	0.737	0.657
$5p\sigma$ $^3\Sigma^+$	–	–	0.723	0.652
$6p\sigma$ $^3\Sigma^+$	–	–	0.714	0.649
$3s\sigma$ g $^3\Sigma^+$	0.15	–	0.161	0.094
$3s\sigma$ $^3\Sigma^+$	0.14	–	0.161	0.102
$3s\sigma$ $^3\Sigma^+$	0.15	–	–	0.104
$3p\pi$ c $^3\Sigma^+$	0.71	–	0.711	0.637
$4p\pi$ $^3\Sigma^+$	–	–	0.655	0.630
$5p\pi$ $^3\Sigma^+$	–	–	0.658	0.627
$6p\pi$ $^3\Sigma^+$	–	–	0.651	0.626

[a] Hammond *et al* (1985).
[b] Ogawa and Ogawa (1974).
[c] Mellinger and Vidal (1995), Mellinger *et al* (1996).

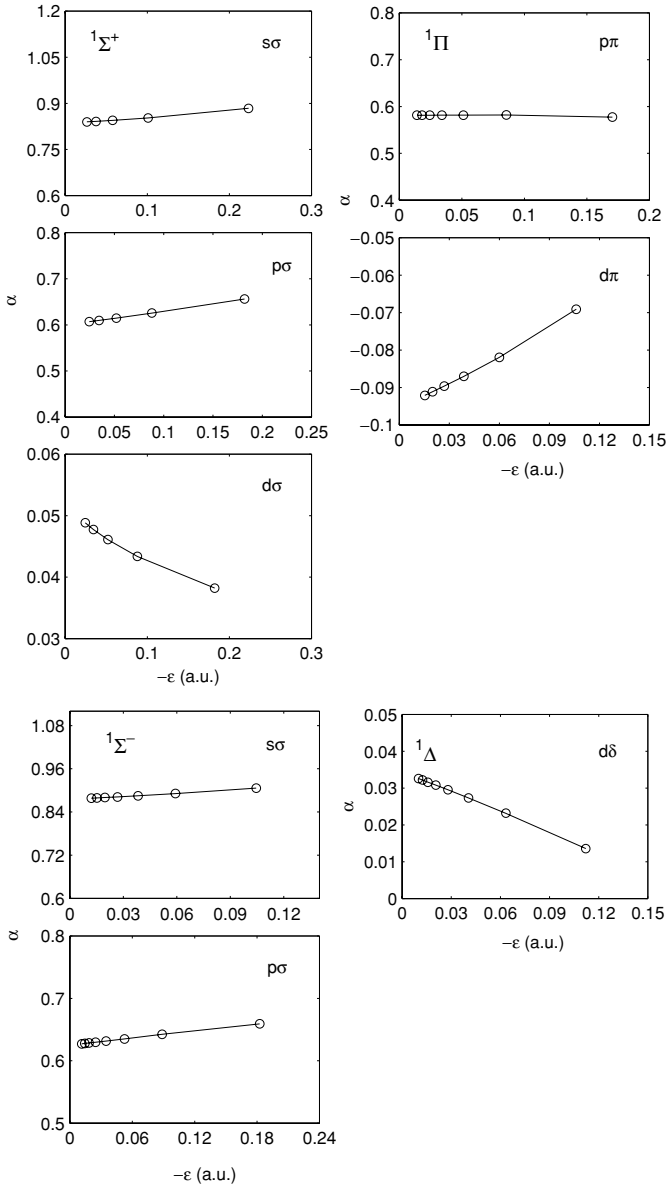

Figure 2. Edlén plots of singlet CO Rydberg states at $R_e = 2.132a_0$. The symmetry of each state is indicated in the panel.

The CO^+ excitation energies for the states $^2\Sigma^+$, $^2\Pi$, $^2\Delta$, $^4\Sigma^+$, $^4\Sigma^-$, $^4\Pi$ and $^4\Delta$ are summarized in table 1. Our model uses the NOs described above and a $(3\sigma,4\sigma, 5\sigma, 1\pi)^9$ CAS-CI. These are compared with the experimental results of Huber and Herzberg (1979) and the CCSDT calculation of Okada and Iwata (2000). The experimental results are in reasonable agreement with our calculation which are somewhat more reliable than those used previously (Tennyson 1996a). Our results lie somewhat higher, but generally not more than 15% higher, than both experiment and the CCSDT calculations. In this context, it should be noted that

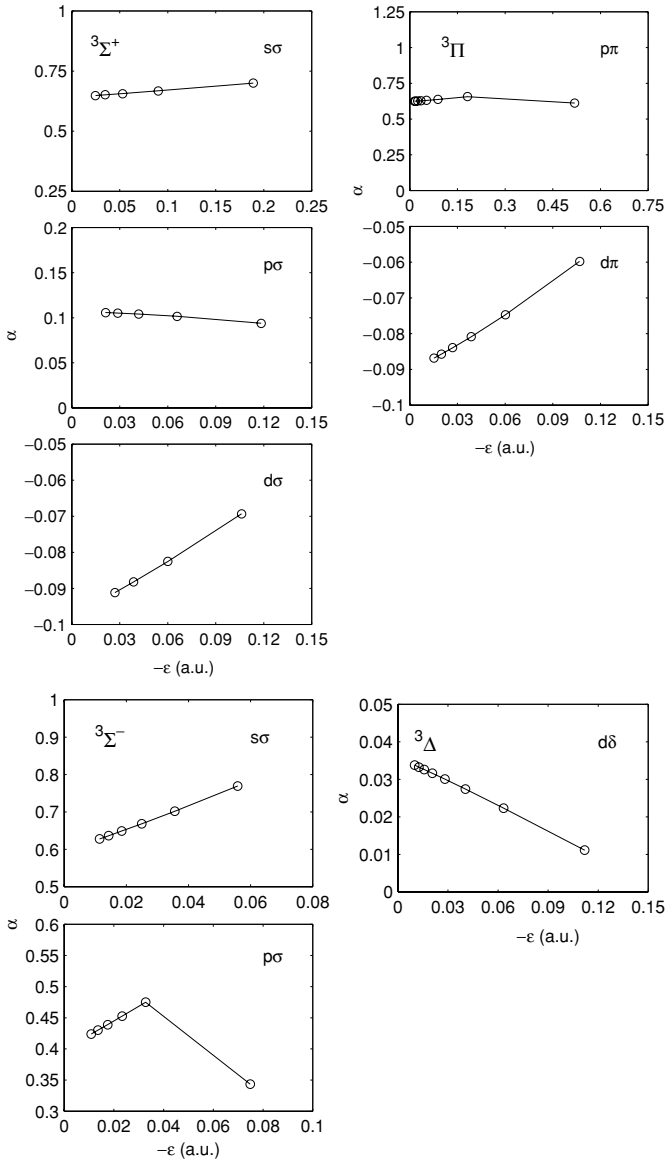

Figure 3. Edlén plots of triplet CO Rydberg states at $R_e = 2.132a_0$. The symmetry of each state is indicated in the panel.

the target calculations used in a scattering calculation do not represent state-of-the-art for electronic structure of the target. This is not so much a computational issue as a question of how a balance can be achieved between more complete N-electron target calculations and the $(N + 1)$-electron scattering calculation; see Tennyson (1996a) for a discussion of this. The issue is further complicated by the requirement that all target calculations use a common set of orbitals as these target states are all coupled in the scattering calculation.

Figure 1 shows the behaviour of the eight lowest states of CO^+ used in our calculation as a function of CO^+ bondlength.

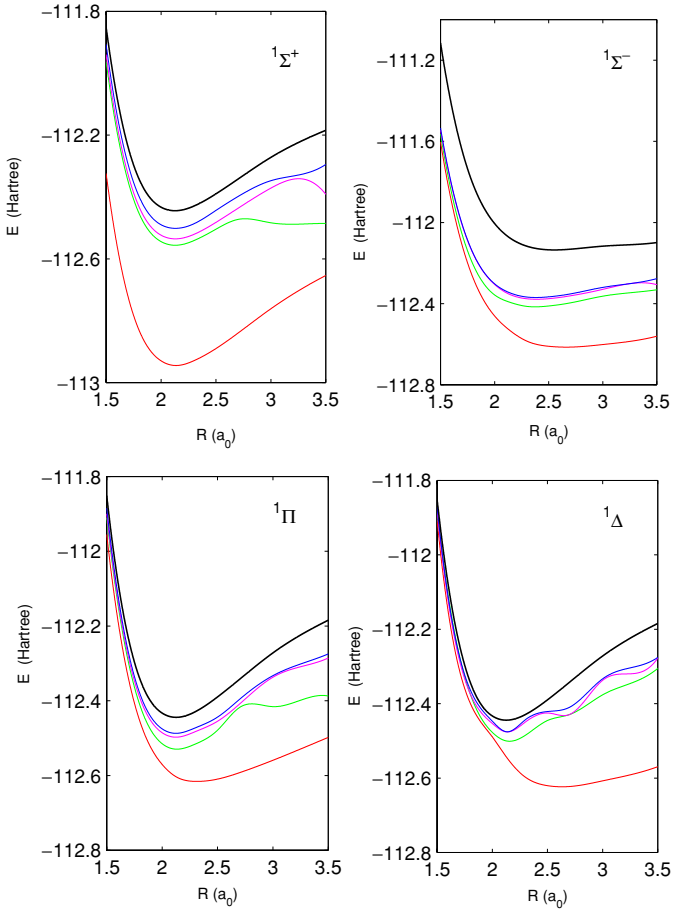

Figure 4. Potential energy curves for the lowest singlet states of the CO molecule. The top most curve (in black) in each figure is the corresponding CO^+ ground state.

2.3. The CO model

Our calculations used 14 CO^+ natural orbitals $(8\sigma, 4\pi, 2\delta)$. These orbitals were augmented by continuum orbitals $F_{i,j}$, expressed as a truncated partial wave expansion around the centre of mass. Partial waves with $l \leqslant 6$ and $m \leqslant 2$ were retained in the expansion. The radial parts of the continuum functions were generated as numerical solutions of an isotropic Coulomb potential. Those solutions with an energy below 10 Ryd were retained. A Buttle (1967) correction was used to correct for the effect of this truncation or, alternatively, the fixed boundary condition used to generate the functions. To correct for linear dependence effects two σ and one π orbitals were removed using Lagrange orthogonalization (Tennyson *et al* 1987). The resulting $62\sigma, 52\pi, 42\delta$ functions were Schmidt orthogonalized to the target NOs.

Calculations were performed using the $(3\sigma,4\sigma, 5\sigma, 1\pi)^9$ CAS target wavefunction for the CO^+ states. Target orbitals not used in the CAS were treated in the same fashion as the continuum functions, $F_{i,j}$ in equation (1), and contracted with the target CI (Tennyson 1996a). All calculations used an R-matrix radius, a, of $10a_0$ except for those performed for a CO bondlength of $3.5a_0$ for which $a = 15a_0$ was used to accommodate larger size of the target.

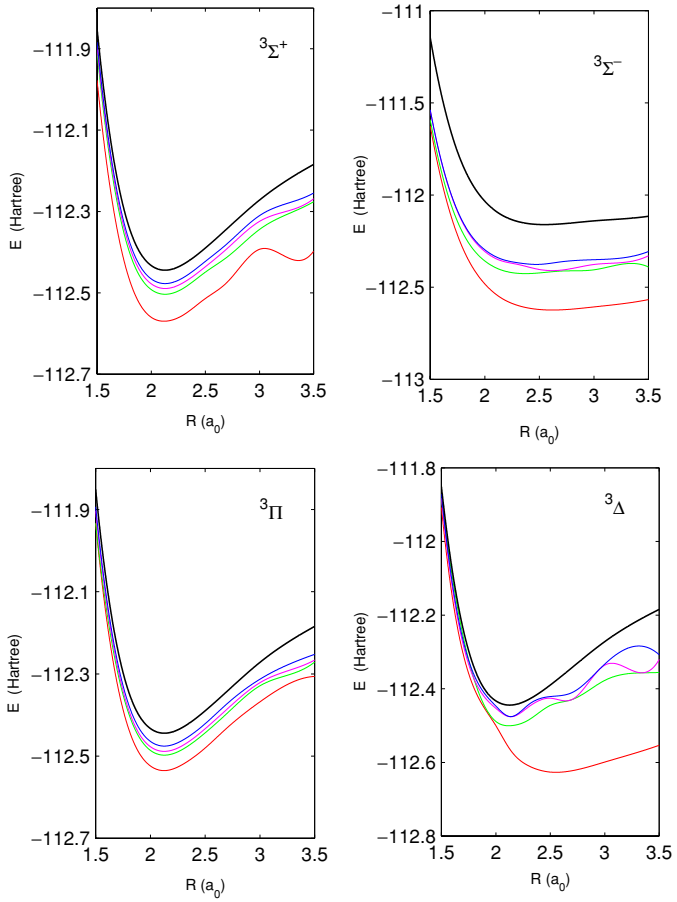

Figure 5. Potential energy curves for the lowest triplet states of the CO molecule. The top most curve (in black) in each figure is the corresponding CO^+ ground state.

Scattering calculations were performed for $^1\Sigma^+$, $^1\Sigma^-$, $^1\Pi$, $^1\Delta$, $^3\Sigma^+$, $^3\Sigma^-$, $^3\Pi$ and $^3\Delta$ total symmetries. Table 2 summarizes the different target states used for each symmetry in the close-coupling expansion of the electron wavefunction, equation (1).

2.4. Bound states

The inner region solutions thus obtained are used to construct an *R*-matrix on the boundary. In the outer region, in addition to the Coulomb potential, the potential was given by the diagonal and off-diagonal dipole and quadrupole moments of the CO^+ target states. The *R*-matrices were propagated (Morgan 1984) in this potential until the wavefunction could be matched with exponentially decreasing functions obtained from a Gailitis expansion (Noble and Nesbet 1984). For the present work the *R*-matrices were propagated to $50a_0$.

Bound states were found using the searching algorithm of Sarpal *et al* (1991) with the improved nonlinear, quantum defect-based grid of Rabadán and Tennyson (1996). Not all target states included in the inner region close-coupling expansions were explicitly treated in

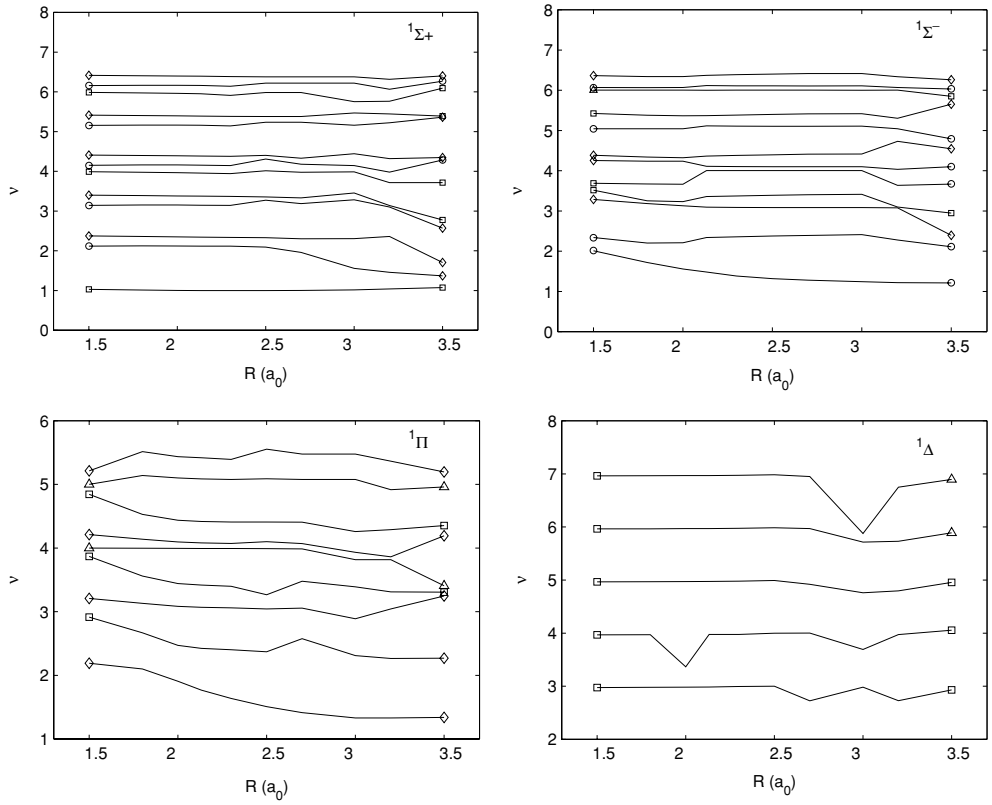

Figure 6. Effective quantum number ν of CO singlet states molecule as a function of bondlength, R. The l character of each states is indicated at the extrema by the following: ○—s state; ◇—p state; □—d state; △—f state; *—g state.

the outer region where the heavily closed channels associated with these states were found to make little quantitative difference, but did prove to be a cause of numerical instability in these calculations.

3. Results

3.1. Rydberg states at equilibrium bondlength

Table 3 compares vertical excitation energies for some of the lower lying electronically states of CO with both experimental estimates and previous calculations. For the lowest-lying states, our method is not as reliable as that of a high accuracy quantum chemistry procedure, such as coupled cluster singles doubles triples (CCSDT), with a large basis such as the calculation by Kucharskii *et al* (2001). However, such methods are not readily extended to treat even fairly low-lying Rydberg series. We note that the more approximate perturbation theory methods employed by Nielsen *et al* (1980) are not variational, unlike our calculations which can be relied upon to give an upper bound to the exact result.

For higher Rydberg states, it is more useful to compare quantum defects rather than excitation energies. Tables 4 and 5 make such a comparison for singlet and triplet states,

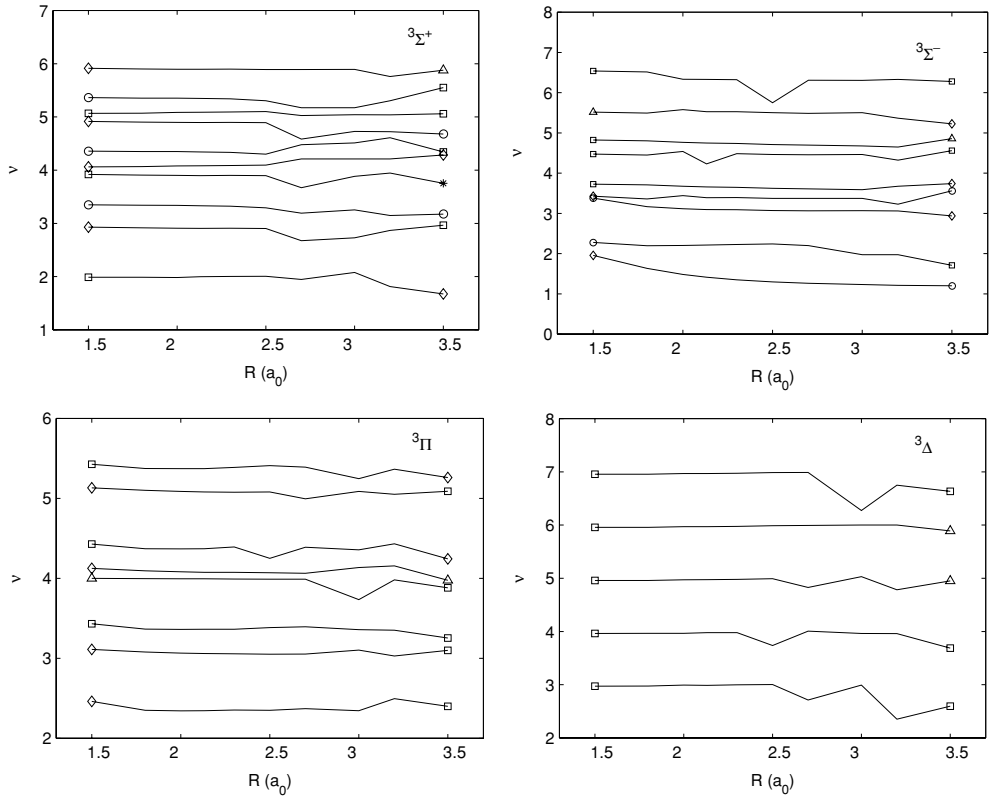

Figure 7. Effective quantum number ν of CO triplet states molecule as a function of bondlength, R. The l character of each states is indicated at the extrema by the following: ○—s state; ◇—p state; □—d state; △—f state; *—g state.

respectively. There are much more reliable data available for the singlet states, so a detailed comparison is worthwhile.

It is apparent that our calculations give results qualitatively similar to those of Hiyama and Nakamura (1996) and Hiyama *et al* (1997), although appears to be more consistent in that in all cases the quantum defects are underestimated by about 0.07. This behaviour is similar to that observed in a previous R-matrix study on Rydberg states of NO Rabadán and Tennyson (1997) which underestimated the quantum defects by closer to 0.05 for all states. The increased error in the case of CO is to be anticipated given that NO^+ is a closed shell whereas CO^+ is not, meaning that the there are greater interactions with the valence electrons.

Another notable result in table 4 is the smooth variation of the calculated quantum defects with respect to the principle quantum number, n, for a given symmetry. This smoothness is not shown by the experimental results which, unlike the fixed bondlength theory calculations, contain some allowance for vibrational motion. This will be discussed further below.

Apart from our previous calculation (Tennyson 1996a), there appears to be no calculated quantum defects for triplet Rydberg states of CO. Less surprisingly the experimental data are also more limited than for the singlet state. However, table 5 also shows that our calculations systematically underestimate the quantum defects by about 0.07.

The behaviour of high-lying Rydberg states is best shown using Edlén (1964) plots. For a particular Rydberg series, these plots compare quantum defect as a function of the energy ϵ, given as

$$\epsilon_{nl\lambda} = -\frac{1}{(n - \alpha_{nl\lambda})^2} \tag{2}$$

where n is the principal quantum number and $\alpha_{nl\lambda}$ is the quantum defect. Figures 2 and 3 show Edlén plots for our quantum defects, with singlet and triplet symmetries respectively, at the CO equilibrium bondlength. These figures show that the quantum defects do vary very smoothly with n and allow estimates to be made for the energy/quantum defect of the many (infinity of) higher states not listed in tables 3–5.

3.2. Rydberg states as a function of bondlength

To obtain potential energy curves for Rydberg states of CO our calculations were repeated for ten bondlengths in the range $1.5 \leqslant R \leqslant 3.5a_0$. The resulting curves for the lower lying states are given in figures 4 and 5 for singlet and triplet states, respectively. All curves except, the ones with Σ^- total symmetry, couple to $X\,^2\Sigma^+$ ground state and are, in general, approximately parallel to this state. However, a number of perturbations, which are in general in the form of avoided crossings, are clearly visible in the figures. The lack of smoothness in the experimentally measured quantum defects as a function of n, as displayed in tables 4 and 5, would appear to be due to the various perturbations of the curves. This suggests that the quantum defects measured will be sensitive to the precise nuclear motion state for which this measurement is made.

A more informative method of considering the behaviour of these Rydberg states as a function of R is to look at the quantum defects. Figures 6 and 7 show this behaviour for the singlet and triplet states, respectively. It is notable that the quantum defects in general show a rather weak dependence of the C–O separation except in the cases where there are localized perturbation caused almost certainly by intruder states.

4. Conclusions

We have calculated potential energy curves and quantum defects for Rydberg states as a function of internuclear separation. Our calculations do not give complete agreement with the experiment, but appear to systematically underestimate the quantum defects by about 0.07 for all symmetries. This information means that our calculations should give a good starting point for the analysis of further spectra of this important molecule.

Acknowledgments

We thank Jimena Gorfinkiel for advice while the calculations were being performed, and the Royal Society and the Indian DST for funding KC's visit to UCL during which this work was performed.

References

Baker J, Tchang-Brillet W-Ü L and Julienne P S 1995 *J. Chem. Phys.* **102** 3956–61

Baluja K L, Mason N J, Morgan L A and Tennyson J 2000 *J. Phys. B: At. Mol. Opt. Phys.* **33** L677–84

Burke P G and Berrington K A 1993 *Atomic and Molecular Processes—An R-matrix Approach* (Bristol: Institute of Physics Publishing)

Buttle P J A 1967 *Phys. Rev.* **160** 719–29
Cade P E and Huo W M 1967 *J. Chem. Phys.* **47** 614
Drabbels M, Heinze J, ter Meulen J J and Meerts W L 1993 *J. Chem. Phys.* **99** 5701–10
Ebata T, Hosoi N and Ito M 1992 *J. Chem. Phys.* **97** 3920–30
Ebata T, Sutani T and Mikami N 1995 *Chem. Phys. Lett.* **240** 357–61
Edlén B 1964 *Handbuch der Physik vol 27* (Berlin: Springer)
Eidelsberg M and Rostas F 1990 *Astron. Astrophys.* **235** 472–89
Eidelsberg M and Rostas F 2003 *Astrophys. J. Suppl.* **145** 89–109
Eikema K S E, Hogervorst W and Ubrachs W 1994 *Chem. Phys.* **181** 217–45
Gianturco F A and Giorgi P G 1996 *Phys Rev.* A **54** 4073–7
Glushkov V N and Theophilou A K 2001 *Phys. Rev.* A **64** 064501
Gutsev G L, Nooijen M and Barlett R J 1998 *Phys. Rev.* A **57** 1646–51
Hammond P, King G C, Jureta J and Read F 1985 *J. Phys. B: At. Mol. Opt. Phys.* **18** 2057–73
Hiyama M and Nakamura H 1996 *Chem. Phys. Lett.* **248** 316
Hiyama M, Kosugi N and Nakamura H 1997 *J. Chem. Phys.* **107** 9370
Huber K P and Herzberg G 1979 *Constants of Diatomic Molecules* (New York: Van Nostrand Reinhold)
Kirby-Docken K and Liu B 1977 *J. Chem. Phys.* **66** 4309–16
Komatsu M, Ebata T, Maeyama T and Mikami N 1995 *J. Chem. Phys.* **103** 31
Kucharskii S, Włoch M, Musiał M and Bartlett R J 2001 *J. Chem. Phys.* **115** 8263
Leyh B and Raseev G 1986 *Phys. Rev.* A **34** 2920–35
Leyh B and Raseev G 1988 *J. Chem. Phys.* **89** 820–9
Masaki T, Adachi Y and Hirose C 1995 *Chem. Phys. Lett.* **139** 62–5
Mellinger A and Vidal C R 1995 *Chem. Phys. Lett.* **238** 31
Mellinger A, Vidal C R and Jungen C 1996 *J. Chem. Phys.* **104** 8913
Mellinger A, Rohwer E G and Vidal C R 2001 *J. Mol. Spectrosc.* **206** 216
Morgan L A 1984 *Comput. Phys. Commun.* **31** 419–22
Morgan L A, Tennyson J and Gillan C J 1998 *Comput. Phys. Commun.* **114** 120–8
Nielsen E S, Jørgensen P and Oddershede J 1980 *J. Chem. Phys.* **73** 6238
Noble C J and Nesbet R K 1984 *Comput. Phys. Commun.* **33** 399–411
Okazaki A, Ebata T and Mikami N 2001 *J. Chem. Phys.* **114** 7886–900
Ogawa M and Ogawa S 1972 *J. Mol. Spectrosc.* **41** 41
Ogawa S and Ogawa M 1974 *J. Mol. Spectrosc.* **49** 454
Okada and Iwata 2000 *J. Chem. Phys.* **112** 1804
Papadopoulos M G, Willets A, Handy N C and Underhill A E 1996 *Mol. Phys.* **88** 1063
Rabadán I and Tennyson J 1996 *J. Phys. B: At. Mol. Opt. Phys.* **29** 3747–61
Rabadán I and Tennyson J 1997 *J. Phys. B: At. Mol. Opt. Phys.* **30** 1975–88
Rescigno T N and Orel A E 1981 *Phys Rev.* A **24** 1267–1271
Rozum I, Mason N J and Tennyson J 2003 *J. Phys. B: At. Mol. Opt. Phys.* **36** 2419–32
Salvini S, Burke P G and Noble C J 1984 *J. Phys. B: At. Mol. opt. Phys.* **17** 2549
Sarpal B K, Branchett S E, Tennyson J and Morgan L A 1991 *J. Phys. B: At. Mol. Opt. Phys.* **24** 3685–99
Singleton L, Brint P and Thomas G P 1995 *J. Chem. Soc. Faraday Trans.* **91** 2699
Tennyson J 1996a *J. Phys. B: At. Mol. Opt. Phys.* **29** 1817–28
Tennyson J 1996b *J. Phys. B: At. Mol. Opt. Phys.* **29** 6185–201
Tennyson J and Noble C J 1984 *Comput. Phys. Commun.* **33** 421–4
Tennyson J, Burke P G and Berrington K A 1987 *Comput. Phys. Commun.* **47** 207–12